Optica Applicata, Vol. XVIII, No. 3, 1988

On the Fraunhofer diffraction on a three-dimensional slit *

A. KULIG, J. SNAKOWSKI

Pedagogical University, Institute of Physics, ul. Rejtana 16, 35–959 Rzeszów, Poland.

TOMASZ WIĘCEK

Technical University, Department of Physics, ul. W. Pola 2, 35–012 Rzeszów, Poland.

This paper deals with the diffraction of light on the slit formed between straight reference edge and the cylindrical metallic surface. In view of metrological application of diffraction patterns, a series of experiments with objects of different radii has been performed. A simple model is discussed to explain obtained experimental data.

1. Introduction

There are numerous suggestions concerning possibility of measurement of small linear dimensions by means of analysis of diffraction patterns [1], [2]. In particular, one can measure separation of two objects by observation of the far-field diffraction pattern resulting from the diffraction of light on a slit aperture formed between a test and reference object. When the width d of the slit is large in comparison with the wavelength λ and its length $l \gg d$, the far-field diffraction pattern intensity distribution is given by the well-known equation

$$I = I_0 \sin \beta^2/\beta^2 \tag{1}$$

where

$$\beta = kd/2 \sin \vartheta, \tag{2}$$

and I_0 is the intensity on the axis, i.e., for the diffraction angle ϑ equal to zero; $k = 2\Pi/\lambda$ stands for the wavenumber.

For given wavelength, one can determine the slit width by determination of minima of intensity which (all equal to zero) are defined by $\beta_n = n\Pi$ ($n = \pm 1, \pm 2, \pm 3, \ldots$) so that

$$d \sin \vartheta_n = n\lambda. \tag{3}$$

---

* This paper is a contribution to the Central Research Program CPBP 02.20.

In practice, at least one of the objects forming the slit has a three-dimensional structure and can no longer be approximated by a sharp edge. Because of asymmetry of the slit formed between a straight reference edge and a three-dimensional test body, one can expect asymmetry in obtained diffraction pattern. This asymmetry, depending on the geometry of the test object and on the optical properties of its surface, will affect, in particular, the position of extrema of the far-field intensity distribution and, in consequence, the accuracy of determination of the slit width. In view of metrological application a series of diffraction experiments was performed with a parallel slit between reference edge and metallic cylindrical surface of varying radius of curvature. To explain obtained experimental results, we propose a simple theoretical model presented in the following.

2. Experimental

For registration of the far-field intensity distribution, an experimental setup presented in Fig. 1 has been used. The beam of monochromatic light ($\lambda = 0.6328$ μm) from He-Ne laser is guided parallel to the experiment table by a system of beam

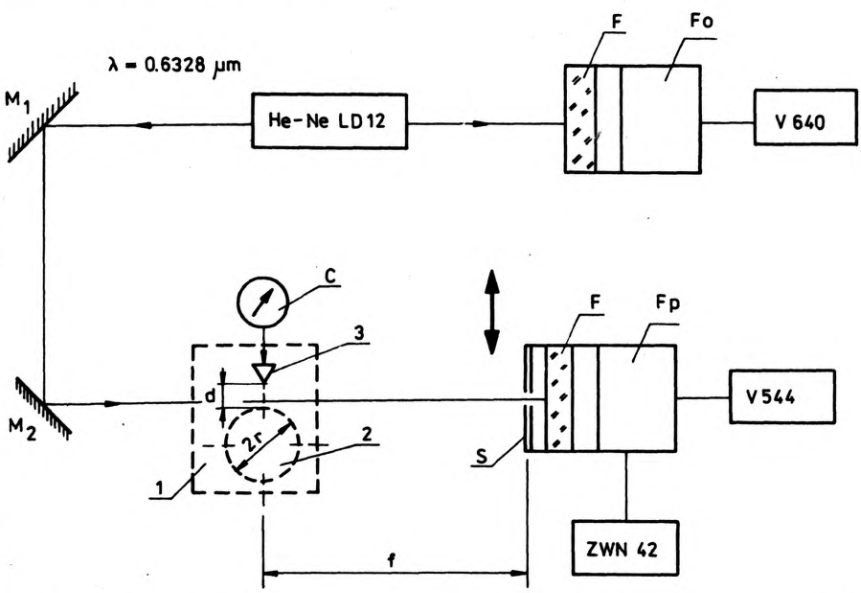

Fig. 1. Scheme of the measuring system: 1 – slit, 2 – cylinder, 3 – edge, C – inductive indicator, S – scanning slit, F – interference filters, Fo – photoelement, Fp – photomultiplier, f – distance of the edge from the scanning slit, V640, V544 – digital voltmeter, M_1, M_2 – beam guiders, ZWN 42 – power supply

guiders M_1, M_2. The total intensity of the beam is controlled by the BPYP 30 photoelement. The width of the examined slit is measured by inductive indicator Fimetr 200. The intensity distribution in the far-field is measured by means of photomultiplier M12FS52A. The detector is provided with vertical scanning slit of

width of 100 μm and can be translated horizontally by means of precision micrometer screw with optical system of reading.

Additional measurements have been performed to establish the geometrical properties of the laser beam in the plane of the object. For the diameter of the Gaussian beam, measured at level I_0/e^2, we obtained $2w > 2$ mm. The divergence angle of the beam has been also measured and evaluated as $2\theta < 7.5 \times 10^{-4}$ rad. By elementary estimation one can prove that for such parameters of the beam neither the density distribution across the beam nor the curvature of the wavefront influence essentially the diffraction pattern, when the slit width is of order of 100–200 μm.

To ascertain that the diffraction we investigate is the Fraunhofer one, the distance between the object and detector must be chosen sufficiently large. In the case of parallel slit the criterion of applicability of the Fraunhofer approximation reads [3]

$$d^2 \ll f\lambda \tag{4}$$

where f is the distance of the point of observation from the aperture. In the presented above setup, we adopted value of $f = 787.8$ mm satisfying the above condition for $d = 140$ μm, which is the slit width used in most of our experiments.

The intensity distribution in the diffraction pattern produced by a single slit formed by two parallel edges is characterized with great dynamics in changes of intensity in successive striae (the values of respective maxima are in proportion: 1:0.047:0.017:0.008...). To obtain faithful spectral characteristics of the slit it is then necessary to adopt a detector displaying linear response within wide range of input signal intensity. The adopted M12FS52A phototube has been tested by its illumination by laser beam through a set of grey filters. The obtained dependence of electric signal on number of applied grey filters is presented in Fig. 2.

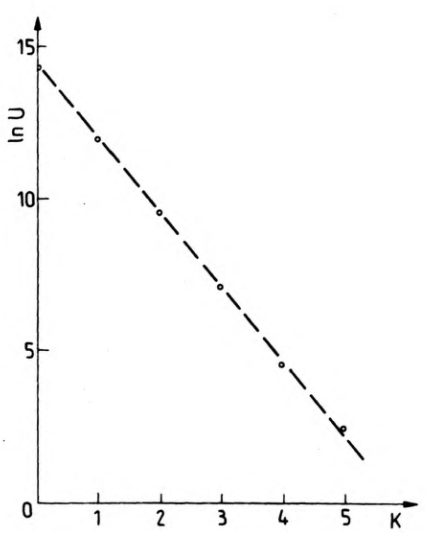

Fig. 2. Phototube linearity test. K denotes number of applied grey filters

The next stage of experiment comprised the alignment of the optical system. The photocathode of the phototube has been set perpendicularly to the direction of propagation of the laser beam. Then, the cylindrical surface of the slit has been positioned parallel to the blade edge by proper setting of angles α and γ (see Fig. 3).

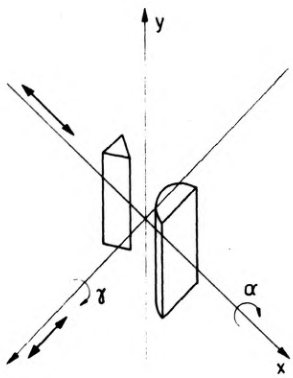

Fig. 3. Alignment of the edge-cylinder system

Central position of the cylindrical surface with respect to the edge has been fixed by means of determination of position characteristics of the blade with the slit being closed. By shifting the cylindrical surface in z-direction we find this way the maximum of the blade position while it is in contact with the central generatrix of the cylinder.

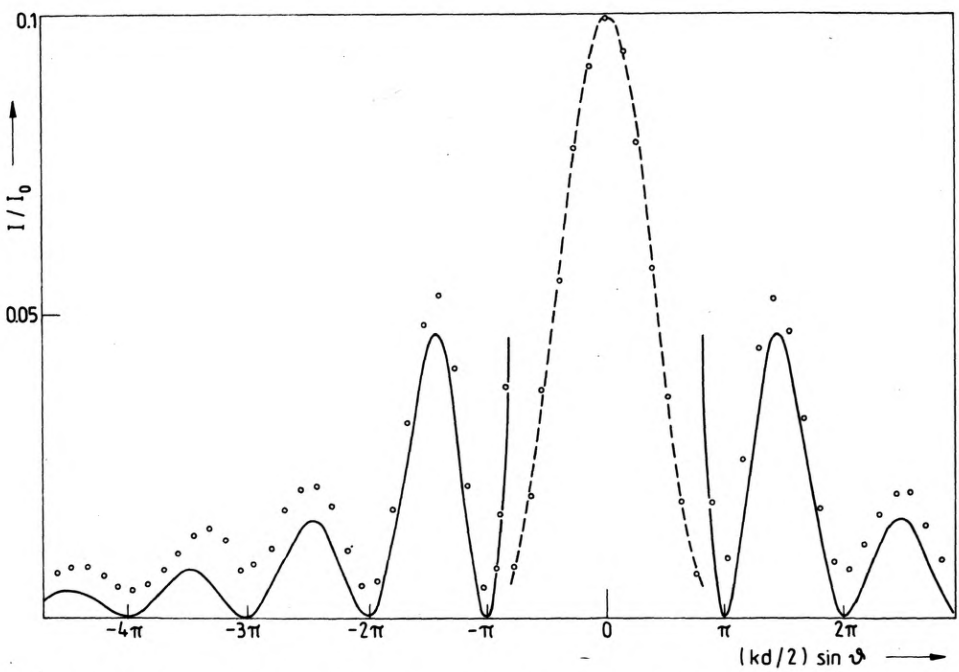

Fig. 4. Diffraction pattern of the planar slit with $d = 140$ μm. The solid line represents theoretical values and points denote results of experiment. The central line of the spectrum is reduced ten times

In the described experimental setup a series of diffraction patterns has been surveyed for different radii of curvature of the metallic cylinder. For verification of the setup first, an experiment with a single parallel slit formed by two blades has been done. The obtained results are shown in Fig. 4. Experimental data are there compared with the theoretical curve representing intensity distribution provided by Eq. (1). The symmetry of the obtained spectrum as well as proper position of extrema confirm pertinence of assumptions concerning properties of the incident wave and applicability of the far-field conditions. It is also evident that the constant component of the scanning detector signal, resulting from internal noise of the phototube, does not alter the position of extrema.

For radii of the test object greater than zero, a systematic shift of the intensity minima has been observed, depending visibly on the radius of the cylinder and quality of the surface. To explain obtained results, a heuristic theoretical model is proposed.

3. Theoretical model

According to the Huygens' principle, each point of the wavefront in an aperture may be considered as a secondary source of wave. The envelope of such secondary waves forms another wavefront. In the case of interest, the wavefront of the incident wave may be assumed as planar in the slit between two parallel thin edges. Instead, when the slit is formed by three-dimensional bodies with light reflecting surfaces, the wavefront will be, in general, distorted. In the case of edge-cylinder aperture there is an undisturbed plane wavefront parallel to the edge and the reflected wavefront. Our task is to find the form of this curved wavefront and the density of distribution of secondary sources on it. Then, to obtain the far-field intensity distribution, one has to summarize contributions arising from secondary sources of both wavefronts.

Assume that the slit between the edge K and the cylindrical reflecting surface W (Fig. 5) is illuminated by monochromatic plane wave. Points of the slit lying on the

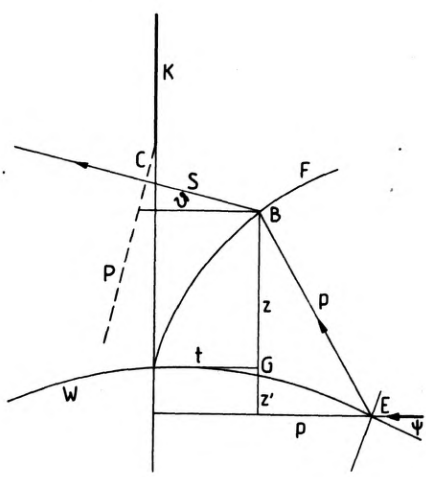

Fig. 5. Construction of the reflected wavefront

extension of K may be treated as sources of secondary wavelets, uniformly distributed and vibrating in phase. The field emitted in the direction defined by angle ϑ is given by

$$V_0(\vartheta) \approx A \int_0^d e^{ik(z-d)\sin\vartheta} dz \tag{5}$$

where z is the distance of the secondary source from the cylindrical surface (see Fig. 5).

As for the reflected wavefront, let us suppose that a ray of light falls on W at point E, explicitly defined by the angle of incidence ψ. After reflection at the same angle ψ, the considered ray reaches point B in the same phase as that of the sources of the slit. Point B belongs then to the wavefront of the reflected wave. If we denote by r the radius of curvature of the cylindrical surface, one can prove that parametric equation of the wavefront is of the form

$$x' = 2r\sin^3\psi,$$
$$y' = r\cos\psi(1+2\sin^2\psi) \tag{6}$$

in Cartesian coordinates of the centre placed in the centre of curvature of cylinder. The wavefront is thus the epicycloid of modulus equal to 1/2.

In order to calculate the contribution of bent wavefront to the field emanating towards direction defined by ϑ, one has to find the phase of secondary wavelets with respect to the plane P. The phase is related to the optical pathlength from point B to C, proportional to their distance S. It can be easily shown by elementary trigonometric calculation that

$$S = (d-z')\sin\vartheta + t\cos\vartheta \tag{7}$$

where

$$z' = r(3\cos\psi - 2\cos^3\psi - 1) \tag{8}$$

and

$$t = 2r\sin^3\psi. \tag{9}$$

The contribution of the bent wavefront is thus given by

$$U_r(\vartheta) \approx AR \int_0^{z''_{\max}} e^{iks(\vartheta,\psi)} dz'' \tag{10}$$

where R stands for reflection coefficient and integration is performed across the reflected beam. Note that

$$z'' = r(1-\cos\psi), \tag{11}$$

and the integration can be performed also over variable ψ. The upper limit of integration is defined by condition expressing the fact of screening of the curved wavefront F by the edge. As it is seen from Fig. 5, the screening can be expressed by

relation

$$t \tan \vartheta > d - z'. \tag{12}$$

Because of complex dependence of variables z and t on z'' (by means of the angular variable ψ), explicit determination of z''_{max} is rather difficult. Although this makes no matter in numerical calculations, let us make some estimation of z''_{max} valid for $\vartheta \ll 1$. Condition (12) can be replaced by a stronger one, $z' > d$, which by Eq. (8) gives (if $\psi \ll 1$)

$$\frac{3}{2}\psi^2 > \frac{d}{r}. \tag{13}$$

Thus, for the incident angle we get the constraint

$$\psi_{max} = [2d/(3r)]^{1/2}. \tag{14}$$

By Eq. (11) we can write approximately $z'' \approx r\psi^2/2$, so that

$$z''_{max} \approx \frac{1}{3}d. \tag{15}$$

In order to calculate the total far-field amplitude and intensity, integrals (5) and (10) have to be added.

4. Results and conclusions

In the experimental setup described above, several measurements have been performed for slits between the edge and cylindrical surfaces of different radii. Figures 6 and 7 present results of the experiment for $r = 5$ mm and $r = 35$ mm, respectively. The solid lines represent values obtained by means of the presented theoretical model. In both cases the value of the reflection coefficient of metallic surface is assumed to be equal to 0.5. As it can be seen from the graphs, in the case of $r = 5$ mm the deviation from the diffraction pattern produced by a single plane slit is of little importance. Nevertheless a characteristic asymmetry occurs, consisting in shift of minima of intensity, and some change of relative intensities of consequent striae is visible. This tendency goes deeply in the case of $r = 35$ mm.

Analysing both diagrams we observe the following characteristic phenomena:

1. The deviation from the diffraction pattern described by Eq. (1) becomes more important with increasing radius of the cylindrical surface. In particular, the minima of intensity are shifted and diffractographic measurement of the slit width is no longer possible with the use of condition (2) defining minima of the single slit diffraction pattern.

2. The shift of minima is different on both sides of the diffraction pattern. On the edge side, the minima occur at lesser values of the diffraction angle than in the case of the simple planar slit of the same width. On the side of the cylinder, minima are shifted towards greater values of ϑ. The greater the radius of curvature of the cylindrical surface, the greater the shift of the minima is.

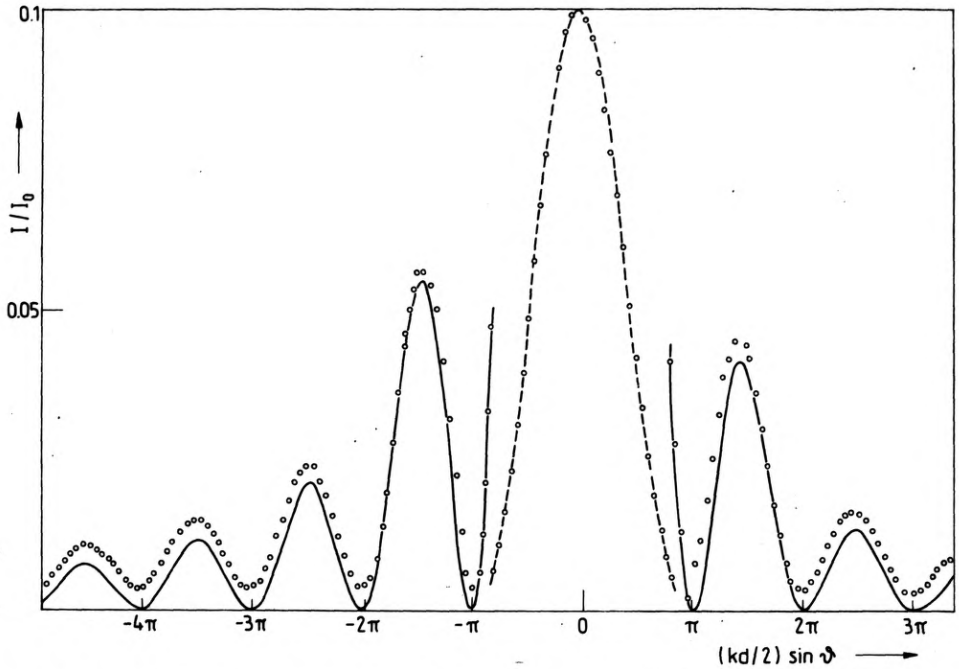

Fig. 6. Diffraction pattern of the edge-cylinder system for $d = 140$ μm and $r = 5$ mm. The solid line represents theoretical values and points denote results of experiment. The central line of the spectrum is reduced ten times

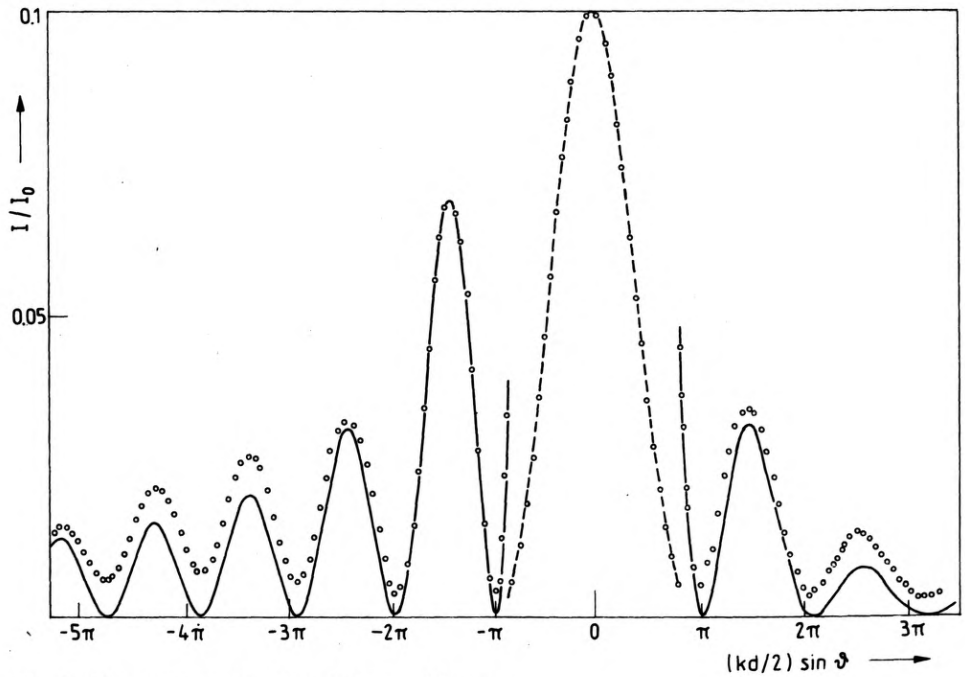

Fig. 7. The same as Fig. 6 but for $r = 35$ mm

3. As for the maxima, their relative values systematically change with varying radius of the cylindrical surface. The striae on the side of the cylinder are weakened, while those on the edge side are intensified. The effect increases with increasing radius of the cylinder. As the problem of relative amplitudes of intensity at individual spectral lines is important in diffractographic detection of linear dimensions by means of spatial filtering, we present the Table in which values of maxima of intensity are given.

Experiment				Model		
n	$r = 0$	$r = 5$ mm	$r = 35$ mm	$r = 0$	$r = 5$ mm	$r = 35$ mm
−4	0.008	0.011	0.015	0.005	0.008	0.015
−3	0.014	0.015	0.026	0.008	0.012	0.020
−2	0.021	0.024	0.032	0.016	0.021	0.031
−1	0.053	0.056	0.066	0.047	0.054	0.073
0	1.000	1.000	1.000	1.000	1.000	1.000
+1	0.053	0.045	0.035	0.047	0.041	0.032
+2	0.021	0.016	0.014	0.016	0.013	0.008

As it can be seen, the effect of reflectance on the three-dimensional slit diffraction pattern is complicated, but variations in positions of minima and intensities of maxima are regular and relatively easy to explain by simple model. The sensitivity of the diffraction pattern shape to the variations of the slit width is of the same type as in the case of simple planar slit. We can therefore say that the application of diffractographic methods to measurement of the width of three-dimensional slit is possible if the shape and reflection properties of the object are well defined.

Acknowledgements — The authors wish to thank Prof. A. Szymański for his helpful and stimulating remarks.

References

[1] PRYOR T. R., HAGENIERS O. L., NORTH W. P. T., Appl. Opt. **11** (1972), 308.
[2] PRYOR T. R., HAGENIERS O. L., NORTH W. P. T., Appl. Opt. **11** (1972), 314.
[3] BORN M., WOLF E., *Principles of Optics*, Pergamon Press, London 1964.

Received December 12, 1986
in revised form March 7, 1988

Дифракция Фраунгофера на трехмерной щели

Настоящая работа касается явления дифракции света на щели созданной прямой гранью и металлической цилиндрической поверхностью. Имея в виду метрологическое применение анализа параметров дифракционного распределения, выполнено ряд измерений для разных значений радиусов цилиндров. Предложена простая теоретическая модель для объяснения полученных экспериментальных данных.